FUNCTIONAL NEURORADIOLOGY

MR imaging and differentiation of cerebral fat embolism syndrome from diffuse axonal injury: application of diffusion tensor imaging

Uttam K. Bodanapally · Kathirkamanathan Shanmuganathan · Nitima Saksobhavivat · Clint W. Sliker · Lisa A. Miller · Andrew Y. Choi · Stuart E. Mirvis · Jiachen Zhuo · Melvin Alexander

Abstract

Introduction Cerebral fat embolism syndrome (CFES) mimics diffuse axonal injury (DAI) on MRI with vasogenic edema, cytotoxic edema, and micro-hemorrhages, making specific diagnosis a challenge. The objective of our study is to determine and compare the diagnostic utility of the conventional MRI and DTI in differentiating cerebral fat embolism syndrome from diffuse axonal injury.

Methods This retrospective study was performed after recruiting 11 patients with severe CFES and ten patients with severe DAI. Three trauma radiologists analyzed conventional MR images to determine the presence or absence of CFES and DAI. DTI analysis of the whole-brain white matter was performed to obtain the directional diffusivities. The results were correlated with clinical diagnosis to determine the diagnostic utility of conventional MRI and DTI.

Results The sensitivity, specificity, and accuracy of conventional MRI in diagnosing CFES, obtained from the pooled data were 76, 85, and 80 %, respectively. Mean radial diffusivity (RD) was significantly higher and the mean fractional anisotropy (FA) was lower in CFES and differentiated subjects with CFES from the DAI group. Area under the receiver operating characteristic (ROC) curve for conventional MRI was 0.82, and for the differentiating DTI parameters the values were 0.75 (RD) and 0.86 (FA), respectively.

Conclusions There is no significant difference between diagnostic performance of DTI and conventional MRI in CFES, but a difference in directional diffusivities was clearly identified between CFES and DAI.

Keywords Magnetic resonance imaging (MRI) · Cerebral fat embolism syndrome (CFES) · Diffuse axonal injury (DAI) · Diffusion tensor imaging (DTI) · Diffusion weighted imaging (DWI)

U. K. Bodanapally (✉) · K. Shanmuganathan ·
N. Saksobhavivat · C. W. Sliker · L. A. Miller · A. Y. Choi ·
S. E. Mirvis · J. Zhuo · M. Alexander
Department of Radiology, University of Maryland Medical Center,
22S Greene Street,
Baltimore, MD 21201, USA
e-mail: ubodanapally@umm.edu

Introduction

Fat embolism syndrome is extremely common after long-bone fractures, but a clinically significant syndrome is manifested in only 0.9–2.2 % of cases [1, 2]. Fat embolism syndrome with neurological manifestations is termed cerebral fat embolism syndrome (CFES) and occurs in up to 60 % of such patients [3, 4]. CFES usually occurs after skeletal trauma in the presence of intravascular fat in the pulmonary and systemic circulation. The syndrome is characterized by clear signs and symptoms [5]. The patient may present with focal neurological signs or generalized encephalopathy varying from drowsiness and confusion to coma [6]. The full neurologic manifestations of fat embolism syndrome usually develop after respiratory insufficiency [4]. Occasionally, the sole manifestation of fat embolism syndrome may be neurologic [7].

MRI is considered the procedure of choice for diagnosing CFES. Specific lesions may present as scattered or confluent areas of vasogenic edema on T2-weighted images [8–10], which may be due to the breakdown of the blood–brain barrier induced by free fatty acids (FFAs), and/or cytotoxic

edema on diffusion weighted images (DWI) consistent with microembolic infarcts and multiple petechial hemorrhages on susceptibility-weighted images (SWI). These lesions usually involve the deep white matter, basal ganglia, corpus callosum, cerebellar hemispheres, and watershed areas [11].

CFES mimics DAI on MRI with similar imaging manifestations of vasogenic edema, cytotoxic edema [9, 10, 12], and micro-hemorrhages, making specific diagnosis a challenge. Because of the treatment implications and risk stratification, it is important to differentiate CFES from DAI. Human brain autopsy has shown both axonal and myelin injury in CFES with injured axons surrounded by damaged and ballooned myelin sheaths [13]. With these histologic findings of axon and myelin pathology, DTI may offer a potential means to evaluate the extent of axon and myelin pathology and assist in differentiation of the two clinical entities.

The purpose of our study was to investigate the diagnostic value of both conventional MRI as well as DTI in differentiating CFES from DAI.

Materials and methods

This retrospective study was compliant with the Health Insurance Portability and Accountability Act and permission was obtained from our institutional review board. The study was conducted at a Level I Trauma Center. The inclusion criteria for this study were (a) presence of clinical signs or symptoms compatible with the diagnosis of fat embolism syndrome according to the Gurd's criteria [14], (b) patients without a history of loss of consciousness after injury (c) normal admission head CT, (d) admission GCS of 15 or 11T (T = tracheal intubation), (some of the patients were intubated for non-neurologic multi-organ trauma and/or pain control in multiple extremity fractures), and a latent, moderate to severe deterioration of GCS to ≤6T. The patients who were intubated, were included only after documentation of a GCS of 15 after resuscitation and tracheal extubation, (e) acquisition of DTI as part of the MRI protocol of the brain (≤18 days after trauma), (f) age ≥18 years and older, regardless of sex. Selection criteria b, c, and d were used to exclude the possibility of an underlying significant traumatic brain injury such as DAI. All the patients had admission head CTs due to the practice pattern at our trauma center, rather than based on clinical evaluation and guidelines for imaging.

Comparison group Ten age, gender, and time to imaging matched patients with moderate to severe DAI (post resuscitation GCS ≤6T) with diffuse micro-hemorrhages comprised the comparison group. Patients with long bone fractures, cortical contusions, and those with deteriorating GCS with a latency period were excluded. We did not select patients with bone fractures in DAI group to exclude the possibility of a rare but real possibility of an associated subclinical or overt CFES.

Reference standard for diagnosis of CFES

An independent reviewer (UB) with 6 years of experience in trauma radiology confirmed CFES based on the presence of the radiological (Table 1; Fig. 1) and clinical criteria (Gurd's criteria for fat embolism). CFES patients without micro-hemorrhages on MRI were excluded from the study. This reviewer was not involved in subsequent blinded review, quantitative analysis, or qualitative analysis of the data set.

MRI protocol and image analysis

MR imaging

All imaging was performed on a 1.5 T Avanto scanner (Siemens Medical Solutions; Erlangen, Germany) with parallel imaging capability. All participants received an MRI scan according to our standard head trauma protocol. The protocol consists of both structural and functional scans. Structural images consisted of axial T2 using turbo spin echo (TE_{eff}/TR/ETL=113/5,900 ms/15, 5 mm slices with 1 mm inter-slice gap, 0.6×0.4 mm in-plane resolution), FLAIR (TE_{eff}/TI/TR/ETL=102/2,500/8,000/13 ms, 5 mm slices with 1 mm inter-slice gap, 1.2×0.9 mm in-plane resolution), volumetric T1 (TE/TR=4.76/11 ms with 20° flip angle, $1 \times 1 \times 2$ mm voxels), and SWI (TE/TR= 40/50 ms with 25° flip angle, $0.5 \times 0.5 \times 2$ mm voxels). DTI images were obtained using a double spin-echo echo-planar imaging technique over a 23 cm (FOV), at an in-plane resolution of 1.79×1.79 mm and a slice thickness of 2 mm (three averages; TE/TR of 95/11,200 ms, parallel imaging acceleration factor of 2). A total of 68 axial images were acquired to cover the brain from the apex to the skull base. Diffusion gradients were sensitized in 6 or 12 collinear directions at an effective b value of 1,000 s/mm^2.

Image processing and analysis

Independently and blinded to clinical information, three trauma radiologists (KS, LM, and NS) with 20, 8, and 1 years of experience reviewed the conventional MR images of the study group and comparison group. The reviewers assessed and recorded the presence of various MRI signs of CFES as listed in Table 1. Based on the MRI signs along with the pattern and distribution of edema and micro-hemorrhages, the reviewers indicated the presence or absence of CFE and DAI.

Table 1 MRI signs of CFES that help in differentiation from DAI

| Nonspecific signs	Specific signs in CFES differentiating it from DAI (Fig. 1)
Confluent or scattered areas of vasogenic edema	Micro-hemorrhages are more numerous and confluent extending into digitate white matter with frequent involvement of gray matter
Confluent or scattered areas of cytotoxic edema	Edema, both vasogenic and cytotoxic is more extensive
Micro-hemorrhages in the white matter > gray matter of cerebrum and cerebellum	Micro-hemorrhages are significantly smaller in size

The DTI images were exported offline and processed using FDT (FMRIB Diffusion Toolbox, FMRIB, Oxford, UK). Images were first corrected for eddy-current-induced image distortion, after which the brain parenchyma was extracted using brain extraction tool available within FSL (FMRIB Software Library, Oxford, UK), and the diffusion tensor was estimated for each voxel [15, 16].

The fractional anisotropy (FA) maps of all patients were first spatially normalized to the standard MNI (Montreal Neurological Institute) space, and then segmented into gray matter, white matter, and CSF maps using SPM5 (Wellcome Department of Imaging Sciences; University College London, UK). Segmented images were visually inspected to confirm accuracy of white matter segmentation results. A tissue probability threshold of 0.75 was used to generate binary masks for each tissue type, which were then used to generate histograms of whole brain white matter mean diffusivity (ADC), fractional anisotropy, axial diffusivity (AD) and radial diffusivity (RD) values. Corresponding mean values were then determined.

Statistical analysis

Results from the three radiologists were pooled and compared with the reference standard for CFES. The sensitivity, specificity, and accuracy of conventional MRI in diagnosing
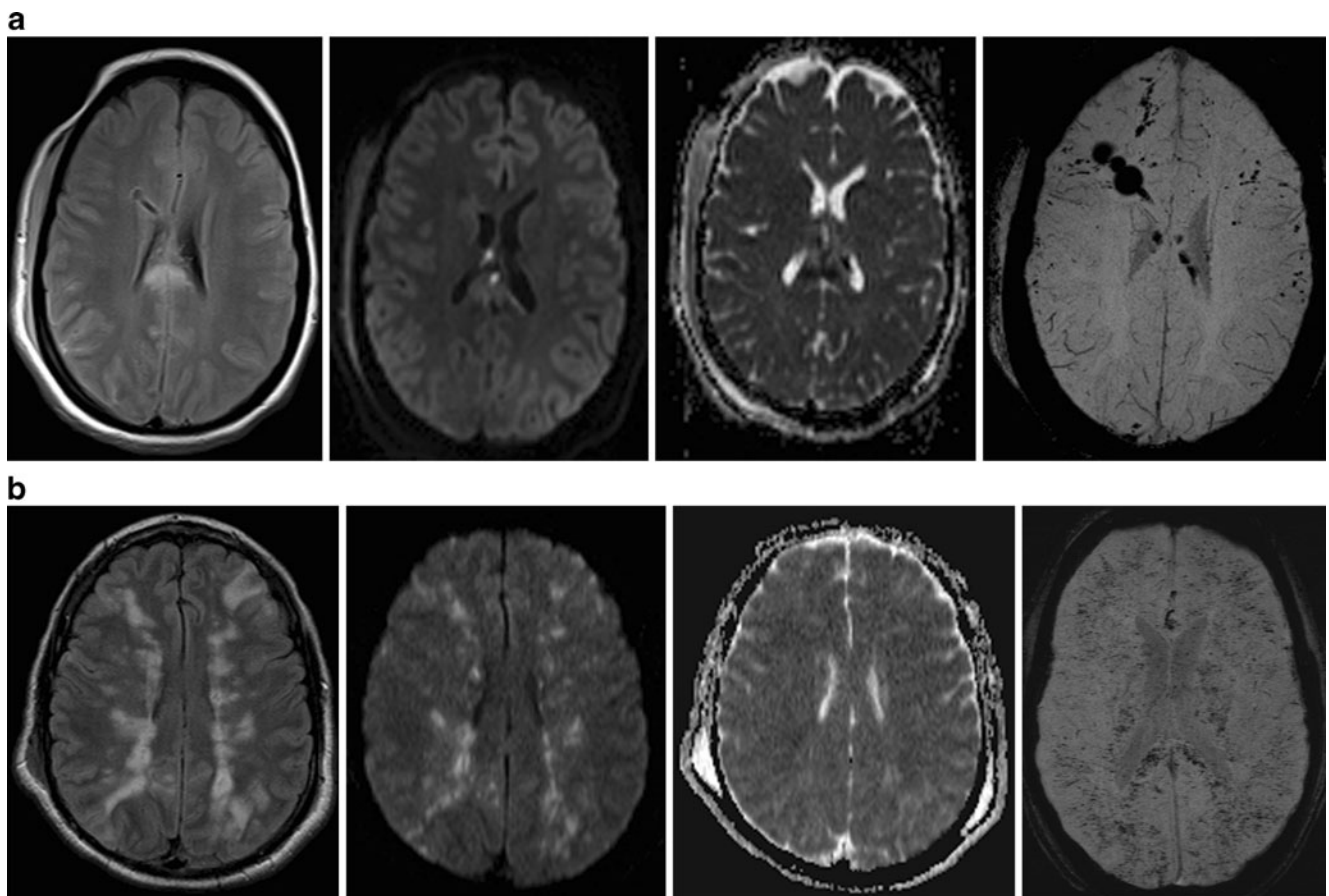
Fig. 1 Examples for conventional images (FLAIR/DWI/ADC/SWI) of DAI and CFES. **a** Images of a patient with DAI with multiple hemorrhages, with both cytotoxic and vasogenic edema in the splenium of the corpus callosum. **b** Images of a patient with CFES with diffuse petechiae, cytotoxic edema, and vasogenic edema after 5 days of admission

CFES and for each of the specific MRI signs of CFES were calculated. Simple interactive statistical analysis (HDS Epimax Table Calculator; Health Decision Strategies LLC, Princeton, NJ) was used for these calculations. Individual radiologist performance was calculated by using prediction profilers.

DTI analysis was conducted using Welch t test for unequal variances. For comparisons between each group, Welch t test was used to assess the difference in AD, ADC, RD, and FA for the whole brain white matter in the two comparison groups. A p value of less than 0.05 was accepted as a statistically significant difference. Statistical analysis was performed using JMP Software (SAS Institute, Cary, NC. versions 9 and 10). Receiver operating characteristic curve analysis was used to evaluate the usefulness of conventional MRI and DTI measurements.

Results

Demographics

A search of the trauma registry using ICD-9-CM diagnostic code 958.1 for fat embolism syndrome from October 2006 to April 2012 yielded 19 patients. The list is cross-matched with our MRI database, which consisted of 17 patients. Two patients without micro-hemorrhages in the brain parenchyma, and four patients with associated traumatic brain injury diagnosed at the time of admission based on GCS were excluded from the study. The medical records of the remaining 11 patients were reviewed for confirmation of CFES based on diagnostic criteria, and constituted our study group. Only four out these 11 patients were prospectively diagnosed as CFES, the rest of the seven patients were misdiagnosed as DAI (sensitivity of 36 %). DTI analysis was performed in ten of the 11 patients. One patient had a follow-up study along with DTI acquisition. All 11 patients had a GCS of 15 or 11T at the time of admission. MRI of the brain was performed in these patients for interval change in mental status along with deteriorating GCS. Demographic, clinical, and imaging characteristics of the study group and comparison group are given in Table 2.

Table 3 Correlations between diffusion parameters in patients with CFES and DAI group

Groups compared	CFES, 95 % CI (μm^2/ms)	DAI, 95 % CI (μm^2/ms)
AD	1.02 (0.99–1.06)	1.03 (0.97–1.08) $p=0.93$
ADC	0.75 (0.72–0.79)	0.72 (0.68–0.76) $p=0.19$
RD	**0.62 (0.59–0.65)**	**0.58 (0.54–0.61) $p=0.03$**
FA	**0.32 (0.3–0.35)**	**0.37 (0.35–0.39) $p=0.002$**

Welch t test was used to assess the difference in directional diffusivities, and statistically significant differences ($p<0.05$) are highlighted in bold

The sensitivity, specificity, and accuracy of conventional MRI in diagnosing CFES obtained from the pooled data are 76, 85, and 80 %, respectively. Various specific signs helped the radiologists in making the correct diagnosis. Innumerable micro-hemorrhages with extensive distribution extending into digitate white matter with frequent involvement of gray matter (sensitivity, 74 %; specificity, 71 %; accuracy, 72 %; and $p=0.007$), extensive cytotoxic and vasogenic edema were found in CFES (sensitivity, 89 %; specificity, 92 %; accuracy, 90 %; and $p=0.002$). Size of the hemorrhages helped in differentiating CFES from DAI, with punctate hemorrhages favoring CFES (sensitivity, 84 %; specificity, 81 %; accuracy, 82 %; and $p<0.001$), while coarse hemorrhages favored DAI (sensitivity, 92 %; specificity, 78 %; accuracy, 86 %; and $p=0.006$). There was no statistical difference in corpus callosum involvement by the micro-hemorrhages between CFES and DAI. The performances of the three radiologists were calculated using the prediction profilers. The probability of predicting CFES based on conventional MRI features were 87, 77, and 80 %, respectively.

Group differences in DTI parameters

Table 3 summarizes the DTI parameters of the whole brain white matter. The DAI group is correlated with the CFES

Table 2 Characteristics of patients in the study group (CFES) and the comparison group (DAI), who underwent diffusion-tensor images as part of MRI of the brain (≤18 days after trauma)

Characteristic	Study group, no. ($n=11$)	Comparison group ($n=10$)
Age, mean (range), year	36 (19–57)	38 (20–53)
Sex (M/F)	8:3	7:3
GCS on admission	GCS 15-seven; GCS 11T-four	GCS <6T
GCS at MRI, Mean (range)	5T (3T–6T)	5T (3T–7T)
Time to MRI after admission, mean (range), day	7 (2–13)	5 (1–16)
Number of patients with fractures	11 (unilateral femur, 8; bilateral femur, 2; tibia, 4; others)	0

GCS Glasgow Coma Scale

group and the respective p values are shown. The statistically significant variables are shown in bold.

Increased RD and decreased FA as predictors of CFES

The mean RD has a higher value in the study group and differentiated subjects with CFES (RD–0.62 μm^2/ms) from DAI subjects in the comparison group (RD—0.58 μm^2/ms, p=0.03; Fig. 2a). Similarly, the mean FA differentiated subjects with CFES (FA=0.32 μm^2/ms) from those without CFES in the comparison group (0.37 μm^2/ms, p=0.002; Fig. 2b).

One follow-up study, which was not included in the analysis showed a progressive increase in RD to 0.696 (day 19) from 0.668 (day 12). However, the FA had also increased to 0.283 from 0.278 along with an increase in AD (1.02 to 1.068) and ADC (0.785 to 0.82).

Receiver operating characteristic curve analysis

The ROC AUC for conventional MRI and the significantly different DTI parameters were 0.82, 0.75 (RD), and 0.86 (FA), respectively. The individual threshold scores for RD

Fig. 2 Scatterplot of **a** RD, **b** FA, for patients with CFES and DAI. *Data points* = individual diffusivities (mm^2/s), *horizontal lines* = associated 95 % confidence intervals
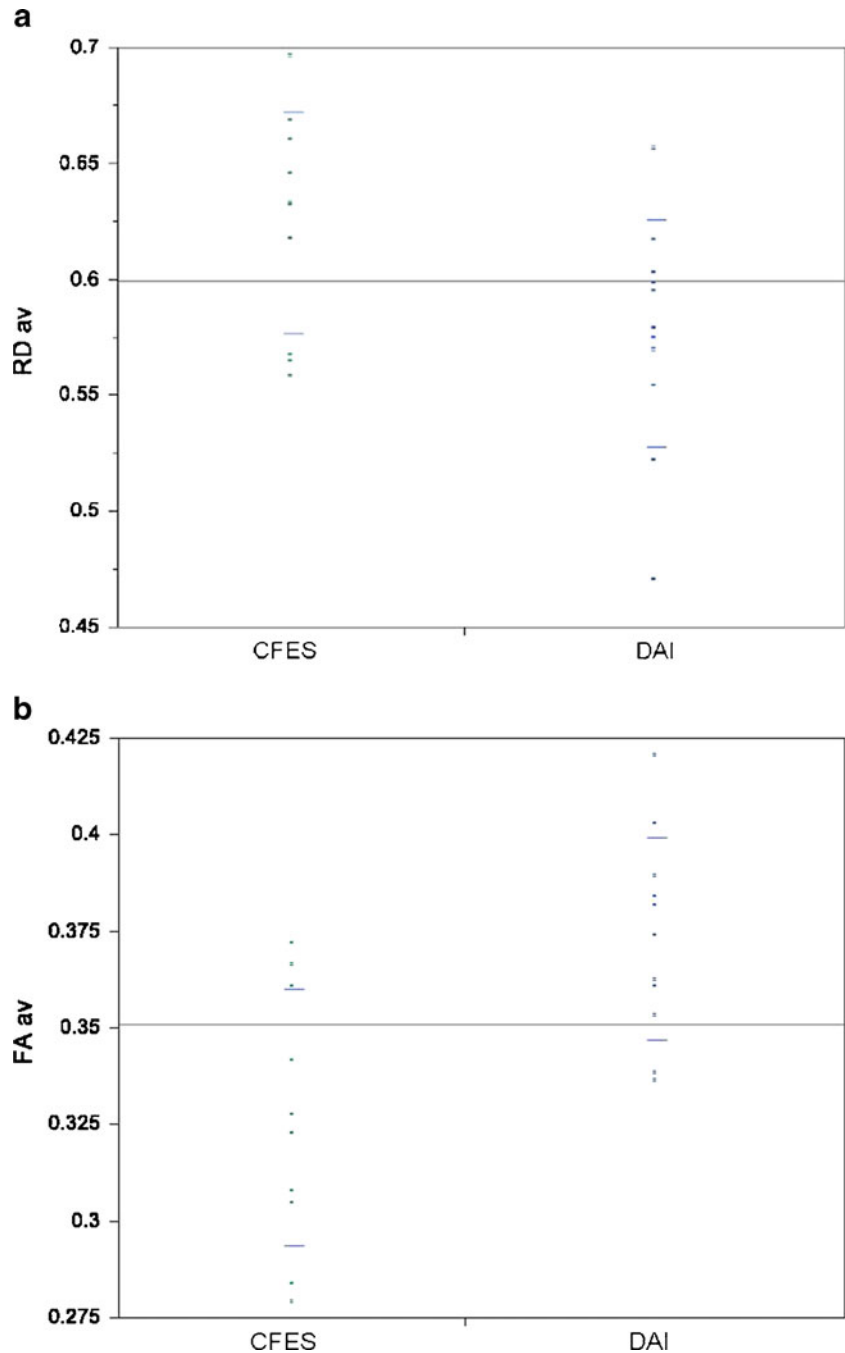
and FA were 0.604 and 0.35 μm^2/ms. Due to the correlation between RD and FA values, there was little additional improvement in AUC by adding the two significantly different measures.

Figure 3 shows the ROC curve for the conventional MRI (3a) and the DTI measurements (3b and 3c). The AUC for mean FA and conventional MRI indicates a good ability of both these tests to correctly discriminate the patients with and without CFES. Mean RD has a fair ability for such discrimination.

There was no statistically significant difference between the performance of DTI (FA) compared to the conventional MRI assessment ($p > 0.05$).

Discussion

In this study, we systematically analyzed the usefulness of conventional MRI and DTI in differentiating CFES from DAI. We found that using conventional MRI findings, the sensitivity was 76 %, specificity 85 %, and accuracy of 80 %. The mean AUC was 0.82. However, the prospective diagnostic sensitivity was much lower for CFES (sensitivity of 36 %); the majority of patients were misdiagnosed as DAI. The significant improvement in the performance is likely from the inherent bias of the retrospective nature of the study. The incidence of severe CFES with MRI manifestations of micro-hemorrhages is a rare disease entity with less than 20 cases identified during the study period of 6 years. This may have limited the experience and awareness of the radiologists to identify CFES on MRI, hence may have rarely considered this disease in the differential diagnosis for micro-hemorrhages during the prospective evaluation. But in our retrospective study, the reviewers were made aware of the radiological features and they systematically used the given signs in differentiating CFES

from DAI. Using DTI analysis, the ROC curves for diagnosing CFES yielded an AUC value of 0.745 for RD and 0.864 for FA values. There was no statistically significant difference between the performance of DTI (FA) compared to conventional MRI in differentiating patients with the presence or absence of CFES in acute and early subacute stages.

The typical findings of CFES at autopsy include diffuse petechiae and ischemic lesions predominantly involving the white matter, with less frequent involvement of gray matter [13]. The ischemic lesions are described as anemic lesions, and are identified as irregular, often spongy areas containing eosinophilic swollen axis cylinders surrounded by ballooned myelin sheaths varying in size from 1–4 mm [13]. Experimental studies have demonstrated an early onset of vasogenic edema invoked by histotoxic effects of FFAs, causing severe vasculitis leading to blood–brain barrier breakdown, vascular rupture, and petechiae [17]. Similar studies have demonstrated the appearance of cytotoxic edema, attributed to small vessel occlusion by fat droplets resulting in ischemic lesions [18].

The increase in RD found in our study may be related to damaged and ballooned myelin sheaths surrounding the axons found at autopsy in decedents with CFES. Increased RD in CFES compared to DAI likely reflects an early onset of myelin damage in CFES, which can be explained by the FFA-induced inflammatory response as shown in experimental studies [17]. The invasion of macrophages may result in active demyelination and myelin thinning. In contrast, RD is expected to remain unchanged in the acute phase of DAI due to absent or minimal loss of myelin sheaths, followed by a gradual increase in RD as myelin thinning along with active demyelination by macrophages progresses during the subacute phase [19]. A significant reduction of FA in CFES, compared to DAI, is expected due to an increase in RD, which
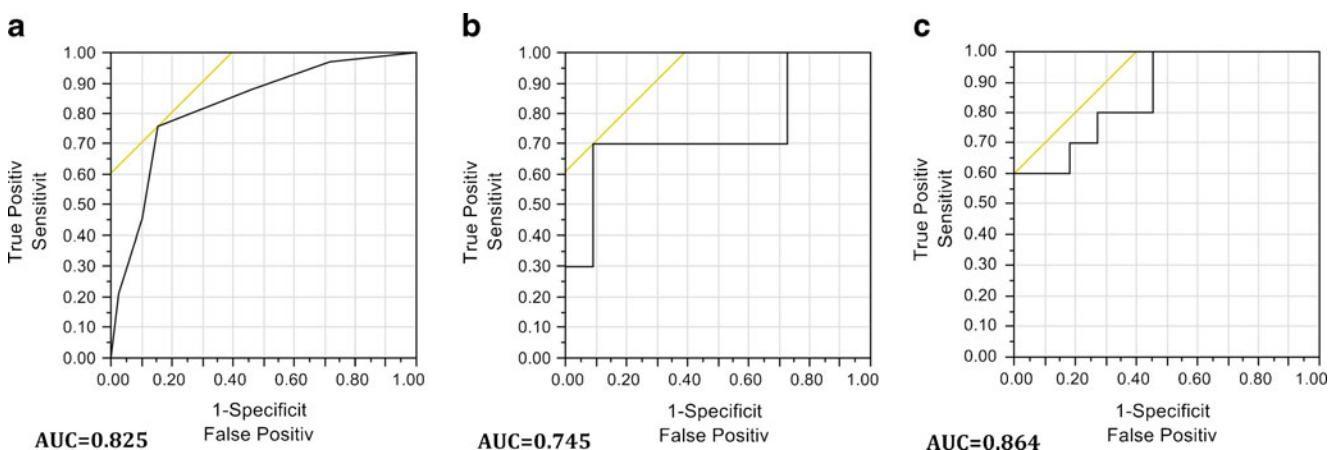
Fig. 3 ROC curves of **a** conventional MRI and **b** RD and **c** FA determining the presence or absence of CFES in the study group and comparison group

reduces barriers of diffusion perpendicular to the predominant fiber direction of the axons. There was no difference in AD and ADC values between the two comparison groups. It has been shown that a decrease in AD is expected due to extensive axonal injury with modest reduction in ADC during the acute phase of DAI [19]. Similarly, the presence of injured axons evident at autopsy in decedents with CFES may explain decreased AD and ADC values in these patients. In addition, with the presence of extensive ischemic lesions in CFES, one would expect a disproportionate reduction in ADC and AD values when compared to DAI, but a concomitant vasogenic edema may have caused pseudo-normalization of these values and may explain the rather modest reduction of these values [20, 21].

Retrogression of cytotoxic edema and the embolized lesions on MR images have been demonstrated and supported by many studies [18]. Light and electron microscopy have shown most lesions resolve after 3 weeks with only focal residual lesions due to infarction and demyelination [18]. These mechanisms can explain the DTI findings in the follow-up study performed in one patient, where AD and ADC continued to increase due to the progressive increase in vasogenic edema [20, 21]. This is demonstrated on MRI by a progressive increase in T2-weighted effects causing increased signal intensity on FLAIR and DWI. The ADC maps, however, showed increasing T2 shine through as the cause of increased signal intensity on DWI. The progressive increase in RD can be explained by continued demyelination and an increase in FA due to the effect of increasing AD.

Our observations clearly showed a difference in DTI parameters between CFES and DAI, but use of these parameters has the same diagnostic performance as that of conventional MRI.

The major limitations of our study were the retrospective nature and the small sample size of CFES, though largest to date. The other limitations involve time variations between the injury, symptom onset, and acquisition of MRI. Variable time span between admission and MR acquisition may be due to varying latency of CFES manifestations, insidious presentation, most notable for its evolving pulmonary, and cerebral and cutaneous manifestations with full neurologic manifestations usually developing after respiratory insufficiency. Other factors also have important role in etiology of CFES, which include the time to orthopedic intervention, type of the procedure etc. These time variations and differences in age and sex may have influenced the DTI parameters, although time to imaging after trauma and age and sex were matched between the study population and the comparison group. Due to a small sample size and a very small dynamic range of GCS scores (one patient with 3T and rest with either 5T or 6T) in the patients with CFES, we could not calculate the correlation between the DTI parameters and GCS scores at MRI scan time.

Conclusion

This study is the first attempt to use DTI imaging in evaluation of CFES. Although there was no significant difference in diagnostic performance of DTI and conventional MRI in CFES, it clearly identified the changes in directional diffusivities that differentiated them from DAI. The changes in DTI parameters may help in understanding the histological differences between the two clinical entities. The increased RD and decreased FA may be due to early onset of myelin damage in CFES compared to DAI. The absence of significant decrease in ADC and AD may be due to the presence of concomitant parenchymal vasogenic edema, in spite of severe diffusion weighted effect on DWI corresponding to cytotoxic edema. DTI yields quantitative parameter providing a more objective measure of severity and prognostic information concerning likely clinical outcomes in various neurologic disorders. It may provide similar information in CFES. The ideal study to evaluate the DTI parameters in mild and moderate forms of CFES and to correlate the values with clinical outcomes would be a prospective controlled study with a large sample size.

References

1. Muller C, Rahn BA, Pfister U, Meinig RP (1994) The incidence, pathogenesis, diagnosis, and treatment of fat embolism. Orthop Rev 23:107–117
2. Parizel PM, Demey HE, Veeckmans G et al (2001) Early diagnosis of cerebral fat embolism syndrome by diffusion-weighted MRI (Starfield Pattern). Stroke 32:2942–2944
3. Pfeffer G, Heran MK (2010) Restricted diffusion and poor clinical outcome in cerebral fat embolism syndrome. Can J Neurol Sci 37(1):128–130
4. Johnson MJ, Lucas GL (1996) Fat embolism syndrome. Orthopedics 19(1):41–49
5. Talbot M, Schemitsch EH (2006) Fat embolism syndrome: history, definition, epidemiology. Injury 37(Suppl 4):S3–S7
6. Jacobson DM, Terrence CF, Reinmuth OM (1986) The neurologic manifestations of fat embolism. Neurology 36(6):847–851
7. Bardana D, Rudan J, Cervenko F, Smith R (1998) Fat embolism syndrome in a patient demonstrating only neurologic symptoms. Can J Surg 41(5):398–402
8. Citerio G, Bianchini E, Beretta L (1995) Magnetic resonance imaging of cerebral fat embolism: a case report. Intensive Care Med 21(8):679–681

9. Stoeger A, Daniaux M, Felber S, Stockhammer G, Aichner F, Zur Nedden D (1998) MRI findings in cerebral fat embolism. Eur Radiol 8(9):1590–1593

10. Takahashi M, Suzuki R, Osakabe Y et al (1999) Magnetic resonance imaging findings in cerebral fat embolism: correlation with clinical manifestations. J Trauma 46(2):324–327

11. Chrysikopoulos H, Maniatis V, Pappas J, Filalithis P, Gogali C, Sfyras D (1996) Case report: post-traumatic cerebral fat embolism: CT and MR findings. Report of two cases and review of the literature. Clin Radiol 51(10):728–732

12. Huisman TA, Sorensen AG, Hergan K, Gonzalez RG, Schaefer PW (2003) Diffusion-weighted imaging for the evaluation of diffuse axonal injury in closed head injury. J Comput Assist Tomogr 27(1):5–11

13. Kamenar E, Burger PC (1980) Stroke 11(5):477–484

14. Gurd AR, Wilson RE (1974) The fat embolism syndrome. J Bone Joint Surg Br 56B(3):408–416

15. Smith SM (2002) Fast robust automated brain extraction. Hum Brain Mapp 17(3):143–155

16. Smith SM, Jenkinson M, Woolrich MW et al (2004) Advances in functional and structural MR image analysis and implementation as FSL. Neuroimage 23 Suppl 1:S208–219

17. Kim HJ, Lee CH, Lee SH (2001) Early development of vasogenic edema in experimental cerebral fat embolism in cats: correlation with MRI and electron microscopic findings. Invest Radiol 36(8):460–469

18. Kim HJ, Lee CH, Lee SH, Moon TY (2003) Magnetic resonance imaging and histologic findings of experimental cerebral fat embolism. Invest Radiol 38(10):625–634

19. Mac Donald CL, Dikranian K, Bayly P, Holtzman D, Brody D (2007) Diffusion tensor imaging reliably detects experimental traumatic axonal injury and indicates approximate time of injury. J Neurosci 27(44):11869–11876

20. Nagesh V, Welch KM, Windham JP (1998) Time course of ADCw changes in ischemic stroke: beyond the human eye! Stroke 29(9):1778–1782

21. Schlaug G, Siewert B, Benfield A, Edelman RR, Warach S (1997) Time course of the apparent diffusion coefficient (ADC) abnormality in human stroke. Neurology 49(1):113–119